Research Article | Vol. 26, No. 22 | 29 Oct 2018 | OPTICS EXPRESS 29353
Optics EXPRESS

Tunable terahertz guided-mode resonance filter with a variable grating period

HYEON SANG BARK AND TAE-IN JEON*

Division of Electrical and Electronics Engineering, Korea Maritime and Ocean University, Busan 49112, South Korea
**jeon@kmou.ac.kr*

Abstract: A variable grating period made of quartz has been applied to fabricate a tunable guided mode resonance (TGMR) filter with transverse-electric (TE) and –magnetic (TM) modes in the terahertz (THz) region. We prepared three TGMR filters with grating periods of 5.0, 3.3, and 1.7 μm/mm over the length of the filter. For the 5.0 μm/mm, the resolution of resonance frequency shift of the $TE_{0,1}$, $TE_{1,1}$, and $TM_{0,1}$ was 3.6, 4.0, and 3.4 GHz/mm, respectively. With a metal slit spacing of 2 mm located in front of the TGMR filter, the movable range of the TGMR was 24 mm, and the resonance frequency could be shifted up to 87, 96, and 82 GHz, where the center frequencies of each resonance were 0.402, 0.579, and 0.460 THz, for the $TE_{0,1}$, $TE_{1,1}$, and $TM_{0,1}$, respectively. Furthermore, because the TGMR and guided mode resonance (GMR) filters are placed independently in the THz beam path, both tunable and fixed resonances can be obtained at the same time in the spectrum.

1. Introduction

The study of filters that operate in the THz region is an important research topic because the data can be utilized in many fields, including THz communication [1], sensor [2], and image applications [3]. Recently, THz filters using parallel-plate waveguides (PPWG) [4–7], grooves [5,8] and metamaterials [9–15] have been actively studied. Various filters, from bandpass to band rejection, can be implemented by passing a THz beam through a photonic crystal with a periodic array, which is on one surface of a PPWG [6]. Since the propagation direction of the THz beam is the same as the array direction of the photonic crystal, it is possible to obtain various filters with excellent characteristics. However, doing so requires precise alignment of the THz beam and the PPWG, and it also requires enough space to couple the THz beam to the waveguide.

At the same time, filters using metamaterials have been extensively studied in the microwave [16] to the optical [17] domains. Because the filter size in the THz region is smaller than that of the microwave region and larger than that of the optical region, metamaterials in the THz region are relatively easier to fabricate in terms of size. Although making a metal pattern on dielectric materials still requires a complex process, THz filters using metamaterials have the advantage of easy alignment because they are positioned perpendicular to the direction of the THz beam.

A tunable THz filter that can change the resonance frequency without having to replace samples is a very important THz device. Generally, three mechanisms have been used to make tunable THz filters [18]. The first one is a tuning circuit. In metamaterials, the electromagnetic behavior can be expressed as an equivalent circuit consisting of induction (L), capacitance (C), and resistance (R) elements. Typically, the resonance frequency, which is controlled by the capacitance with voltage [10,11] and a structural gap [12], can be represented as a parallel LC or tank RLC circuit. The second approach is material tuning. Tunable devices can be obtained by controlling the properties of materials, such as permittivity, permeability and conductivity. Tunable THz resonance studies have realized material tuning using temperature [13], optical beam power [14], and magnetic field [15]. The

#344744 https://doi.org/10.1364/OE.26.029353
Journal © 2018 Received 31 Aug 2018; revised 12 Oct 2018; accepted 18 Oct 2018; published 25 Oct 2018

Optics EXPRESS

third mechanism is geometrical tuning. When a part of the filter device is geometrically moved, the resonance is shifted due to a change in phase inversion [7] or structural deformation [19]. Using the relative positions of photonic crystals [20,21] and PPWG [7,22] have been reported as methods to obtain a tunable THz filter. Specifically, the PPWG obtained 6.28 GHz/μm resolution by controlling the gap of the PPWG [7]. Although tunable THz filters using PPWG have good resolution, they still have spatial size and alignment problems. The first and second mechanisms have been applied to many metamaterials. Because it modulates the metal pattern electronically, it has the advantage of being able quickly to tune the resonant frequency. However, because the metal patterns on the dielectric material reflect the incident THz beam, metal patterns reduce transmittance and increase manufacturing cost.

Many optically tunable filters using GMR have been studied using the first and second mechanisms, for example, by adjusting incident angle [23,24], polarization [25], temperature [26], and beam power [27]. We propose a new tunable THz notch filter using the geometrical tuning method with a TGMR filter composed of an all-dielectric material like quartz. The resonance frequency can be changed continuously by moving the position of the TGMR filter with respect to the incident THz beam. Also, it is easy to align the TGMR filter because the THz beam direction is perpendicular to the filter, like most metamaterial setups. The TGMR filters based on dielectric materials have high transmission rates and high Q-factors, but the tunable speeds have physical limits.

2. TGMR filter design

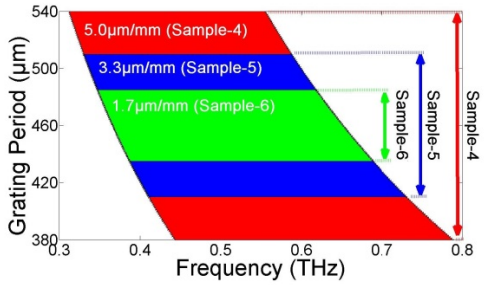

Fig. 1. The region where resonance of the first mode exists according to frequency and grating period (Λ). The vertical arrows indicate the grating period ranges of sample-4, −5, and −6 as shown in Table 1.

Table 1. Specifications of GMR filters.

Period	Sample-1	Sample-2	Sample-3	Sample-4	Sample-5	Sample-6
Top (μm)	400	460	520	385	410	435
Middle (μm)	400	460	520	460	460	460
Bottom (μm)	400	460	520	535	510	485
Period variation (μm/mm)*	0.0	0.0	0.0	5.0	3.3	1.7
Last groove angle (°)	0.0	0.0	0.0	11	7	4

*Period variation indicates period difference between top and bottom divided by the length of sample (30 mm)

Diffraction and guiding are the two major physical mechanisms of a GMR filter with a grating made of an all-dielectric material. When a THz wave is incident on the GMR filter, diffraction is produced by the grating. In order to guide the diffracted electric fields within the filter substrate, the effective dielectric constant of the guided mode has to be greater than the dielectric constant of the incident media (air) and less than the average dielectric constant of the filter. Therefore, the conditions for GMRs are given by Eq. (1) [28–30].

$$\sqrt{\varepsilon_{inc}} \le \left| \sqrt{\varepsilon_{inc}} \sin\theta_{inc} - m\frac{c}{f \cdot \Lambda} \right| < \sqrt{\varepsilon_{avg}}, \quad (1)$$

Optics EXPRESS

where ε_{avg} is the average dielectric constant of the GMR filter, ε_{inc} is the dielectric constant of the incident material, m is the m th diffraction mode, and c, f, and Λ are the speed of light, frequency, and grating period, respectively.

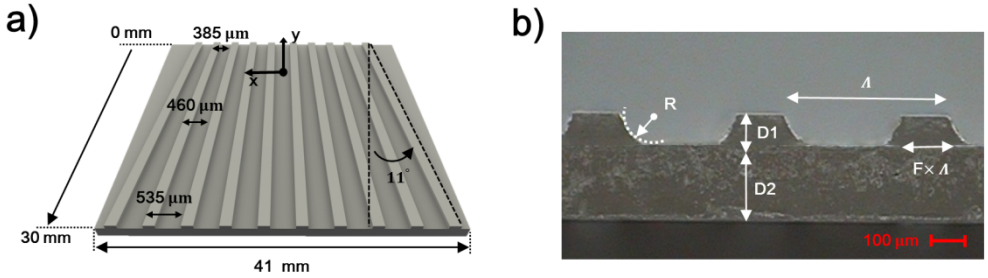

Fig. 2. (a) Schematic diagram of TGMR filter (sample-4). Each grating pattern consists of a groove height (D1) of 60 μm, substrate thickness (D2) of 168 μm, and a filling factor (F) of 32% as shown in the insert figure. The number of grooves is 76. The grating period gradually increases from top to bottom, from 385 μm to 535 μm. The grating period in the middle is 460 μm. The last and first grooves are tilted by ±11° from the center groove, respectively. (b) Cross section photo of the enlarged GMR filter with a grating period of 460 μm. The "R" indicates the inner corner radius of the groove.

When a THz wave from the air is incident perpendicularly ($\theta_{inc} = 0$) to a GMR filter made of quartz, which has a refractive index of 1.95 in the THz region, the region in which the resonance of the first mode (m = ± 1) exists is determined by frequency and grating period, as shown in Fig. 1(a). The resonance frequency region depending on each grating period can only exist in the area painted with color, according to the condition in Eq. (1). As the grating period becomes shorter, the resonance frequency shifts to a high frequency region. We prepared six samples made of quartz as shown in Table 1. Sample-1, –2, and –3 are GMR filters with a constant grating period and 65 grooves, however, sample-4, –5, and –6 are TGMR filters with periods varying per unit length, of 5.0, 3.3, and 1.7 μm/mm with 76 grooves, respectively. The vertical arrows in Fig. 1 indicate period ranges for sample-4, –5, and-6 which were designed for the TGMR filter. Sample-4, –5, and –6 have a trapezoidal shape because the grating period at the bottom is longer than the grating period at the top. However, the middle grating period of all samples is equal to 460 μm.

Figure 2(a) shows a schematic diagram of sample-4. The last and first grooves are tilted by ±11° from the center groove, respectively. Figure 2(b) shows the cross section photo of the filter. Each grating pattern consists of a groove height (D1) of 60 μm, substrate thickness (D2) of 168 μm, and a filling factor (F) of 32%. In Eq. (1), ε_{avg} is related to the filling factor and is independent of the groove height. Therefore, the heights of all the samples were fixed at 60 μm because the change of the resonance frequency with the height of the groove was insignificant. However, during the etching process (prepared by Buysemi Co.), the inner corners of the grooves were rounded, as shown in Fig. 2(b). The radius of the rounded corner causes the resonance frequency difference, compared to the simulated result for the TM mode resonance.

3. Experimental result

3.1 GMR filter measurement

THz time-domain spectroscopy (THz-TDS) was used to characterize the performance of the GMR filters. In our photoconductive THz-TDS system [31], the GMR filters were located in between two parabolic mirrors. The THz wave is incident vertically from the air onto the GMR filters. An ideal GMR filter requires an infinite number of grooves to achieve a strong resonance depth in spectrum [32]. However, due to the limited THz beam, with a diameter of

Optics EXPRESS

2.5 cm, and the GMR filter size, only a finite number of periods are covered by the THz beam. To overcome this limitation, the THz beam transits two identical filters. The grating period is an important parameter of the GMR filter when determining the resonance frequency, as shown in Eq. (1).

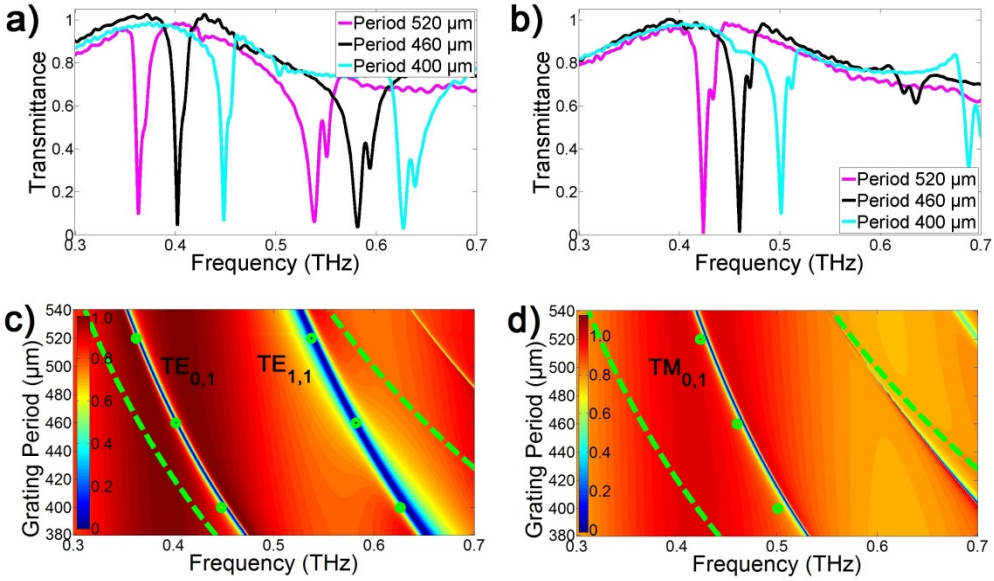

Fig. 3. Transmittance measurement for 400, 460, and 520 μm grating periods. (a) TE mode. (b) TM mode. Simulation image of resonance frequency shift according to grating period. The dots and dashed lines indicate the measured resonance frequencies and the boundary of the region where the first mode resonance exists, as shown in Fig. 1. (c) TE mode. (d) TM mode.

Figures 3(a) and 3(b) show the measured transmittance of the TE and TM modes for 400, 460, and 520 μm grating periods for sample-1, –2, and –3, respectively. Each sample has two strong TE modes which can be expressed as $TE_{0,1}$ and $TE_{1,1}$ where the $TE_{1,1}$ mode can be removed by increasing the dielectric constant of the incident material [24]. The electric field distributions of the first and second resonance are guided modes of half and full wave across the samples, respectively. These electric field distributions indicate TE_0 and TE_1 modes, with the first subscript denoting the field distributions for the guided modes in the slab waveguide (substrate of sample). The second subscript of the mode expression denotes the number of the mode diffracted by the grating. Like the TE mode, the first strong TM mode is represented by the $TM_{0,1}$ mode, which indicates a half wave field distribution in the slab waveguide and the first diffraction mode by the grating.

Because the THz beam waist between the two parabolic mirrors is at the focal length of the first parabolic mirror, the incident THz beam cannot be perfectly perpendicular to the two filters, which are 8 cm apart from each other. Therefore, a small side lobe resonance occurred at each resonance. Due to the multiple reflections by the GMR filters, the base lines of the measured transmittances do not approach to 1 and have a large oscillation in the spectrum. However, the resonance depths using the two filters approach maximum value (the transmittance approaches 0). The resonance frequencies of the measured $TE_{0,1}$ modes were 0.363, 0.402, and 0.448 THz for periods of 520, 460, 400 μm, respectively. As the grating period decreases, the resonance frequency shifts to higher frequency, because the grating period and the resonance frequency were inversely proportional. The measured resonance frequencies of other modes ($TE_{1,1}$ and $TM_{0,1}$) were also shifted to the high frequency region as the grating period decreased.

Optics EXPRESS

Finite difference frequency domain (FDFD) simulation imags for the TE and TM modes of the GMR are shown in Figs. 3(c) and 3(d), respectively. The solid lines and dots indicate the simulated and measured resonance frequencies for different grating periods, respectively. The dashed lines indicate the boundary of the region where the first mode resonance exists as shown in Fig. 1. All of the measured resonance frequencies are in this region. The experimental and simulation results of the TE modes are in good agreement, but the TM mode is slightly different. This is because the polarization of the THz beam in the TE mode is incident horizontally on the grooves, but the TM mode is incident vertically on the grooves. Therefore, the TM mode is more sensitive to the rectangular shape of the groove than the TE mode. Furthermore, the inner corners of the groove are not as perfect as in the simulations, as can be seen in Fig. 2(b). Therefore, the measured and simulated resonance frequencies of the TM mode are in less agreement than the TE mode.

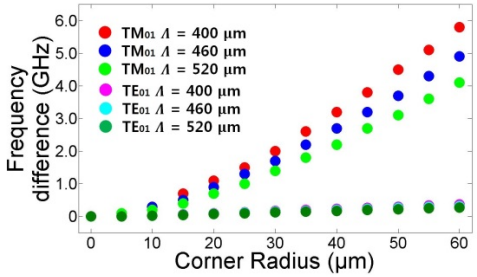

Fig. 4. Resonance frequency difference between rectangular inner corner radius (R = 0) and rounded inner corner radius.

Figure 4 shows the simulation results of the difference in resonance frequency between the rectangular inner corner radius (R = 0) and rounded inner corner radius, shown as "R" in Fig. 2(b). We simulated the difference in resonance frequency of $TE_{0,1}$ and $TM_{0,1}$ for the GMR filters. In the $TE_{0,1}$ mode, there is almost no difference in frequency difference as the inner corner radius increases. However, in $TM_{0,1}$ mode, the frequency difference increases exponentially as the inner corner radius increases. The shorter grating period is more sensitive to the geometric structure of the groove in the grating than the longer grating period. This phenomenon was also observed by measurements. The differences in frequency for the measured and simulated $TM_{0,1}$ mode were 11.2, 6.5, and 6.1 GHz at 400, 460 and 520 μm, respectively. Although the inner corner radius cannot be defined in the fabricated samples because the corner is not a perfectly rounded shape, the frequency difference becomes larger as the grating period becomes shorter as shown in the Fig. 3(d).

3.2 TGMR filter measurement

The TGMR filter is designed so that the grating period can be selected depending on where the THz beam passes. If the THz beam width is too large, the full width half maximum (FWHM) of the measured resonance is widened because the variation range of the grating period is too large. In other words, as the THz beam width continues to decrease, the FWHM of the resonance also continuously decreases. However, when the THz beam width is too small, the noise increases and the resonance is distorted because the THz beam passing through the TGMR filter is too small.

Optics EXPRESS

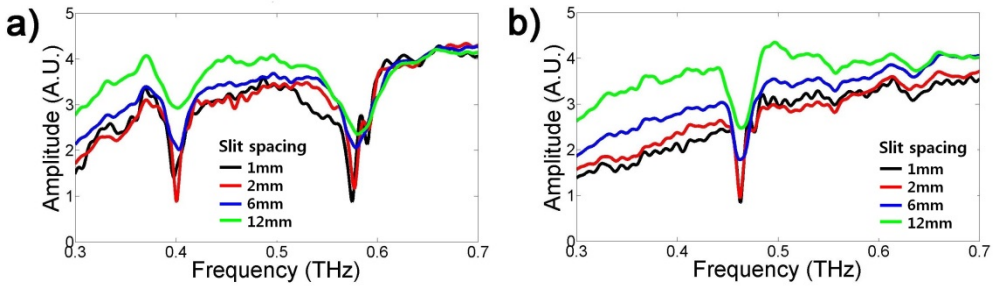

Fig. 5. The amplitude of spectrum near the resonance frequency with different slit spacing. a) TE mode b) TM mode.

It is important to know the optimal THz beam width without increasing noise and resonance distortion. When a rectangular metal slit is located in front of the TGMR filter, the THz beam width passing through the slit is the same as the slit spacing. Therefore, the width of the THz beam passing through the TGMR filter can be adjusted by controlling the slit spacing. Figure 5 shows the amplitude of spectrum near the resonance frequency dependent on the slit spacing for sample-4. When the slit spacing is 12 mm, the FWHM of the resonance is too large. Also, when the slit spacing is 1 mm, the noise increases and the resonance is distorted. We found that the most appropriate spacing was when the slit spacing was 2 mm. We then investigated the characteristics of the TGMR with 2mm fixed slit spacing.

In order to measure resonance frequency shift in the TE and TM modes, the TGMR filter was placed behind a metal slit with 2 mm spacing, as shown in Figs. 6(a) and 6(b), respectively. To measure TE and TM modes the filter moved in the + y and + x directions at 2 mm step intervals for each TGMR filter, respectively. We used a compact motorized translation stage to move the TGMR filter 2 mm for each measurement. Because of scattering at the edge of the filter, the filter movement was from 3 mm to 27 mm over a length of 30 mm as shown in Fig. 2(a). It was found that the $TE_{0,1}$ and $TE_{1,1}$ mode resonances shifted almost linearly to the low frequency region as the grating period increased, as shown in Fig. 6(c), which illustrates the transmittance for sample-4 (5.0 μm/mm). The resonance shift ratios for the filter movement of $TE_{0,1}$ and $TE_{1.1}$ were 3.6 and 4.0 GHz/mm, which correspond to resonance shifts of 0.72 and 0.80 GHz/μm for the grating period variations, respectively. After the slit and filter were rotated 90 degrees counterclockwise, the resonance shift of the $TM_{0,1}$ mode could be measured, as shown in Fig. 6(d). Like the TE modes, the resonance shifted to the low frequency region as the grating period increased. The resonance shift ratios for the filter movement of $TM_{0,1}$ was 3.4 GHz/mm, which corresponds to a resonance shift of 0.68 GHz/μm for grating period variations. We confirmed that these ratios were very similar to the simulation results for each GMR filter with a different period.

Figure 6 (e-g) shows the resonance frequency shift according to the filter movement of the TGMR filters for $TE_{0,1}$, $TE_{1,1}$, and $TM_{0,1}$ of sample-4, −5, and −6, respectively. Sample-4 is most sensitive to the shift. The total resonance frequency shifts of sample-4 were 86.6, 96.2, and 81.8 GHz, which correspond to resolutions of 3.6, 4.0, and 3.4 GHz/mm, for the $TE_{0,1}$, $TE_{1,1}$, and $TM_{0,1}$ modes, respectively. Although the total resonance frequency shifts for sample-6 (1.7 μm/mm) were as narrow as 27.6, 28.1, and 25.0 GHz, it had the best resolutions, which were 1.2, 1.2, and 1.0 GHz/mm for $TE_{0,1}$, $TE_{1,1}$, and $TM_{0,1}$, respectively.

To change the resonance frequency, the GMR filter has to be replaced. However, with the TGMR filter, the resonant frequency can be easily changed by adjusting the position of the filter. Furthermore, it is also possible to selectively use a filter with a sensitive resonance shift, or a filter with a resonance shift that has good resolution. The biggest advantage is that the GMR filters are made of all dielectric materials, which have very low absorption in the

Optics EXPRESS

THz region. Unlike metamaterials with metal patterns on a dielectric substrate, multiple GMR filters only produce a small reflection loss from the material.

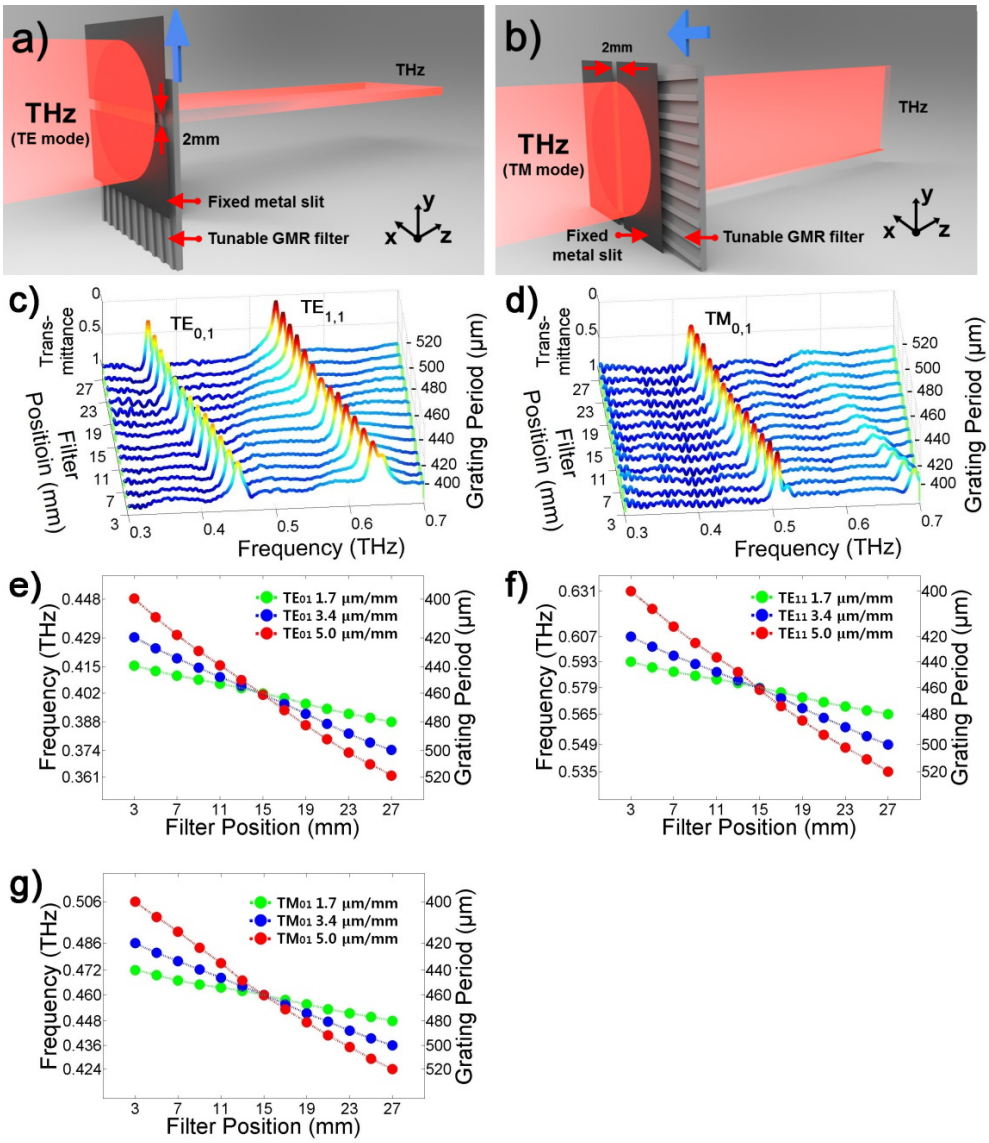

Fig. 6. Schematic diagram of the TGMR filter setup for (a) TE mode and (b) TM mode measurement. Transmittance measurement using the TGMR filter (sample-4) for (c) TE mode and (d) TM mode. Measured resonance frequency shift according to the TGMR filter movement (filter position to center of slit) for (e) $TE_{0,1}$ mode, (f) $TE_{1,1}$ mode, and (g) $TM_{0,1}$ mode. The frequency and grating period scales on the y axis indicate the end points of each data.

We used the TGMR and GMR filters to make double resonances in each mode. As shown in Figs. 7(a) and 7(b), the GMR filter (sample-2) was fixed behind the TGMR filter (sample-4) with a 2 mm slit spacing. When the vertically polarized THz beam enters the TGMR filter, resonance occurs at the THz frequency satisfying the guiding condition, but the THz wave of the other frequencies passes through the TGMR filter. If the period of the fixed GMR filter is different from the period of the TGMR filter, a second resonance occurs in the other

Optics EXPRESS

frequency. When the TGMR filter is moved as shown in the arrow direction, the resonance of each mode shifts from the high frequency to the low frequency region. However, because the GMR filter with a 460 μm uniform period is fixed, the resonance frequencies are also fixed at 0.4021, 0.5823, and 0.4625 THz $TE_{0,1}$, $TE_{1,1}$, and $TM_{0,1}$ as shown in Figs. 7(c) and 7(d), respectively. These fixed resonance frequencies can be utilized as reference frequencies of the double resonances.

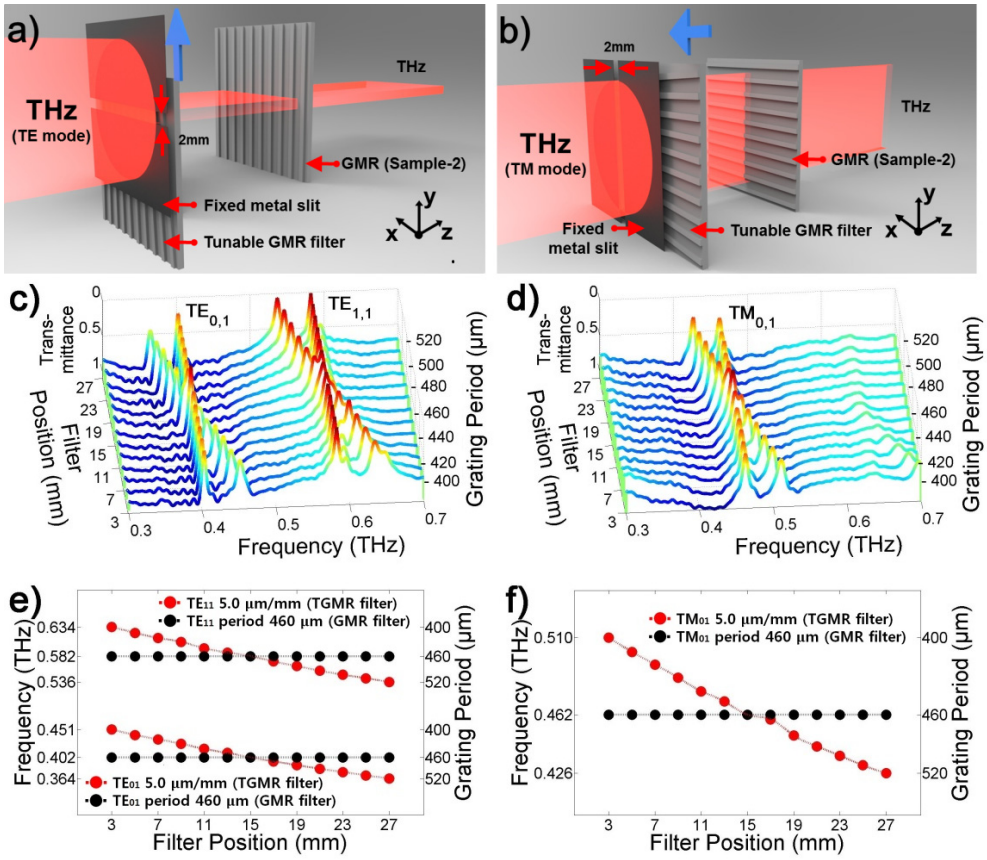

Fig. 7. Schematic diagram of TGMR and GMR filter setup for (a) TE mode and (b) TM measurement. Transmittance measurement using TGMR and GMR filters for (c) TE mode and (d) TM mode. Measured resonance frequency shift with movement of the TGMR filter (filter position) for (e) TE mode and (f) TM mode. The frequency and period scales on the y axis indicate the end points of each data.

Figures 7(e) and 7(f) show the shift in the peak resonance frequencies of the TE and TM modes in Figs. 7(c) and 7(d), respectively, due to movement of the TGMR filter. The shift in resonance frequency produced by the TGMR filter is tunable by changing the filter's position, however, the resonance frequency induced by the GMR filter is fixed. The total resonance frequency shifts in the TGMR filter are 87, 98, and 84 GHz for the $TE_{0,1}$, $TE_{1,1}$, and $TM_{0,1}$ modes, respectively. The tunable range using the TGMR filter position is very similar to the case with a single TGMR filter, as shown in Fig. 6. Because it can simultaneously measure reference (fixed) resonances and tunable resonances, it can be very useful for THz spectroscopy and THz communications.

Optics EXPRESS

4. Summary and conclusions

Compared to the THz transmittance characteristics of a metamaterial, the all-dielectric GMR filter has many advantages. Fabricating metamaterials with metal patterns on the surface of a dielectric material involves a complicated process and high cost. Furthermore, the metamaterial has high reflection loss because of the high refractive index of metal. The resulting low transmittance limits the application of metamaterials. In contrast, an all-dielectric GMR filter has a simple low cost process with low reflection loss.

In this research, we first demonstrate a tunable THz resonance using a TGMR filter which continuously changes its grating period. The resonance frequency can be selected by simply moving the filter with respect to a metal slit of 2 mm. The proposed method in this study is a much simpler and quicker method of changing the resonant frequency than replacing GMR filters with different grating periods. Furthermore, by simultaneously using a TGMR and GMR filter, the design allows tunable dual resonance for the TE and TM modes, with a tunable resonant frequency and a fixed resonance frequency.

In conclusion, because the proposed TGMR filter has a tunable resonance frequency, it has potential for THz applications in spectroscopy, modulators, image sensors, and filters for THz communications in the future.

Funding

National Research Foundation of Korea (NRF), the Korea Government (MSIP) (Grant No. 2016R1A2B4012523).

References

1. J. Ma, N. J. Karl, S. Bretin, G. Ducournau, and D. M. Mittleman, "Frequency-division multiplexer and demultiplexer for terahertz wireless links," Nat. Commun. **8**(1), 729 (2017).
2. X. Hu, G. Xu, L. Wen, H. Wang, Y. Zhao, Y. Zhang, D. R. S. Cumming, and Q. Chen, "Metamaterial absorber integrated microfluidic terahertz sensor," Laser Photonics Rev. **10**(6), 962–969 (2016).
3. Y. Wen, D. Jia, W. Ma, Y. Feng, M. Liu, L. Dong, Y. Zhao, and X. Yu, "Photomechanical meta-molecule array for real-time terahertz imaging," Microsyst. Nanoeng. **3**, 17071 (2017).
4. E. S. Lee and T.-I. Jeon, "THz filter using the transverse-electric (TE_1) mode of the parallel-plate waveguide," J. Opt. Soc. Korea **13**(4), 423–427 (2009).
5. E. S. Lee, J.-K. So, G.-S. Park, D. Kim, C.-S. Kee, and T.-I. Jeon, "Terahertz band gaps induced by metal grooves inside parallel-plate waveguides," Opt. Express **20**(6), 6116–6123 (2012).
6. E. S. Lee, S.-G. Lee, C.-S. Kee, and T.-I. Jeon, "Terahertz notch and low-pass filters based on band gaps properties by using metal slits in tapered parallel-plate waveguides," Opt. Express **19**(16), 14852–14859 (2011).
7. E. S. Lee and T.-I. Jeon, "Tunable THz notch filter with a single groove inside parallel-plate waveguides," Opt. Express **20**(28), 29605–29612 (2012).
8. Y. J. Zhou and B. J. Yang, "Planar spoof plasmonic ultra-wideband filter based on low-loss and compact terahertz waveguide corrugated with dumbbell grooves," Appl. Opt. **54**(14), 4529–4533 (2015).
9. M. Gil, J. Bonache, and F. Martín, "Metamaterial filters: A review," Metamaterials (Amst.) **2**(4), 186–197 (2008).
10. H.-T. Chen, W. J. Padilla, J. M. O. Zide, A. C. Gossard, A. J. Taylor, and R. D. Averitt, "Active terahertz metamaterial devices," Nature **444**(7119), 597–600 (2006).
11. H.-T. Chen, W. J. Padilla, M. J. Cich, A. K. Azad, R. D. Averitt, and J. Antoinette, "A metamaterial solid-state terahertz phase modulator," Nat. Photonics **3**(3), 148–151 (2009).
12. J. Li, C. M. Shah, W. Withayachumnankul, B. S.-Y. Ung, A. Mitchell, S. Sriram, M. Bhaskaran, S. Chang, and D. Abbott, "Mechanically tunable terahertz metamaterials," Appl. Phys. Lett. **102**(12), 121101 (2013).
13. J. Han and A. Lak, "Semiconductor split-ring resonators for thermally tunable, terahertz metamaterials," J. Mod. Opt. **56**(4), 554–557 (2009).
14. H.-T. Chen, J. F. O'hara, A. K. Azad, A. J. Taylor, R. D. Averitt, D. B. Shrekenhamer, and W. J. Padilla, "Experimental demonstration of frequency-agile terahertz metamaterials," Nat. Photonics **2**(5), 295–298 (2008).
15. J. Han, A. Lakhtakia, and C.-W. Qiu, "Terahertz metamaterials with semiconductor split-ring resonators for magnetostatic tunability," Opt. Express **16**(19), 14390–14396 (2008).
16. K. Bi, W. Zhu, M. Lei, and J. Zhou, "Magnetically tunable wideband microwave filter using ferrite-based metamaterials," Appl. Phys. Lett. **106**(17), 173507 (2015).
17. J.-B. Brückner, J. Le Rouzo, L. Escoubas, G. Berginc, O. Calvo-Perez, N. Vukadinovic, and F. Flory, "Metamaterial filters at optical-infrared frequencies," Opt. Express **21**(14), 16992–17006 (2013).
18. J. P. Turpin, J. A. Bossard, K. L. Morgan, D. H. Werner, and P. L. Werner, "Reconfigurable and tunable metamaterials: a review of the theory and applications," Int. J. Antennas Propag. **2014**, 429837 (2014).

Optics EXPRESS

19. H. Tao, A. C. Strikwerda, K. Fan, C. M. Bingham, W. J. Padilla, X. Zhang, and R. D. Averitt, "Terahertz metamaterials on free-standing highly-flexible polyimide substrates," J. Phys. D Appl. Phys. **41**(23), 232004 (2008).
20. T. D. Drysdale, R. J. Blaikie, and D. R. S. Cumming, "Calculated and measured transmittance of a tunable metallic photonic crystal filter for terahertz frequencies," Appl. Phys. Lett. **83**(26), 5362–5364 (2003).
21. T. D. Drysdale, I. S. Gregory, C. Baker, E. H. Linfield, W. R. Tribe, and D. R. S. Cumming, "Transmittance of a tunable filter at terahertz frequencies," Appl. Phys. Lett. **85**(22), 5173–5175 (2004).
22. R. Mendis, A. Nag, F. Chen, and D. M. Mittleman, "A tunable universal terahertz filter using artificial dielectrics based on parallel-plate waveguides," Appl. Phys. Lett. **97**(13), 131106 (2010).
23. M. J. Uddin and R. Magnusson, "Efficient guided-mode-resonant tunable color filters," IEEE Photonics Technol. Lett. **24**(17), 1552–1554 (2012).
24. H. S. Bark, G. J. Kim, and T.-I. Jeon, "Transmission characteristics of all-dielectric guided-mode resonance filter in the THz region," Sci. Rep. **8**(1), 13570 (2018).
25. M. J. Uddin, T. Khaleque, and R. Magnusson, "Guided-mode resonant polarization-controlled tunable color filters," Opt. Express **22**(10), 12307–12315 (2014).
26. M. J. Uddin and R. Magnusson, "Guided-mode resonant thermo-optic tunable filters," IEEE Photonics Technol. Lett. **25**(15), 1412–1415 (2013).
27. D. W. Dobbs and B. T. Cunningham, "Optically tunable guided-mode resonance filter," Appl. Opt. **45**(28), 7286–7293 (2006).
28. L. Rayleigh, "On the dynamical theory of gratings," Royal Soc. **79**(532), 399–416 (1907).
29. S. S. Wang and R. Magnusson, "Theory and applications of guided-mode resonance filters," Appl. Opt. **32**(14), 2606–2613 (1993).
30. J. H. Barton, R. C. Rumpf, R. W. Smith, C. Kozikowsk, and P. Zellner, "All-dielectric frequency selective surfaces with few number of periods," Prog. Electromagnetics Res. B **41**, 269–283 (2012).
31. T.-I. Jeon and D. Grischkowsky, "Characterization of optically dense, doped semiconductors by reflection THz time domain spectroscopy," Appl. Phys. Lett. **72**(23), 3032–3034 (1998).
32. R. R. Boye and R. K. Kostuk, "Investigation of the effect of finite grating size on the performance of guided-mode resonance filters," Appl. Opt. **39**(21), 3649–3653 (2000).